

Aggregation-induced emission nanofiber as dual sensor for aromatic amine and acid vapors

Pengchong Xue,^{a,b*} Jipeng Ding,^b Yanbing Shen,^b Hongqiang Gao,^b Jinyu Zhao,^b Jingbo Sun,^b Ran Lu^b

^a Tianjin Key Laboratory of Structure and Performance for Functional Molecules, Key Laboratory of Inorganic-Organic Hybrid Functional Material Chemistry, Ministry of Education, College of Chemistry, Tianjin Normal University, Tianjin, 300387, P.R. China. *E-mail: xuepengchong@126.com

^b College of Chemistry, Jilin University, 2699# Qianjin Street, Changchun, 130012, P. R. China.

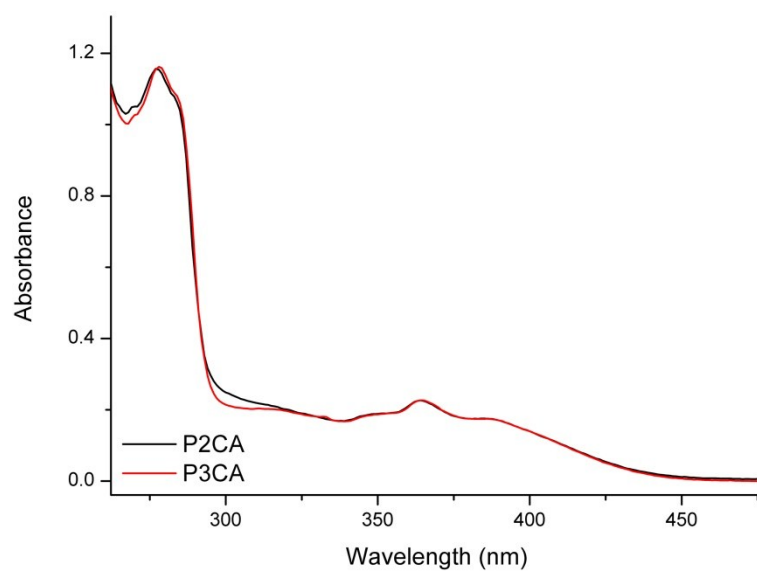


Fig. S1 UV-vis absorption spectra of PC2VA and PC3VA in THF (10^{-5} M).

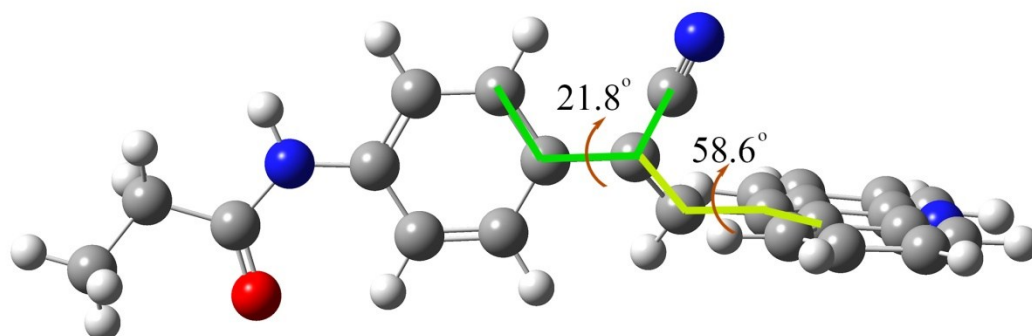


Fig. S2 Optimized conformation of fluorophore with dihedral angles.

Table S1. Gelation abilities of two compounds in organic solvents.^a

| Solvent | PC2VA | PC3VA |
|--------------------------------------|----------|----------|
| cyclohexane | I | I |
| toluene | G (1.3) | PG |
| <i>o</i> -dichlorobenzene | G (1.4) | G (1.8) |
| chlorobenzene | G (1.0) | G (1.3) |
| ethylbenzene | PG | G (3.2) |
| xylene | G (1.8) | PG |
| mesitylene | G (7.3) | PG |
| ethanol | P | G (1.7) |
| <i>n</i> -butanol | P | G (1.7) |
| <i>n</i> -octanol | P | G (4.1) |
| methanol | TG (1.8) | TG (1.4) |
| <i>t</i> -butanol | P | G (2.0) |
| 1,4-dioxane | P | G (2.4) |
| CH ₂ ClCH ₂ Cl | P | G (1.3) |
| benzyl alcohol | G (10) | S |
| DMF | S | S |

^a G: gel; I: insoluble; S: soluble; TG: turbid gel; CGC is the critical gelation concentration (mg/mL).

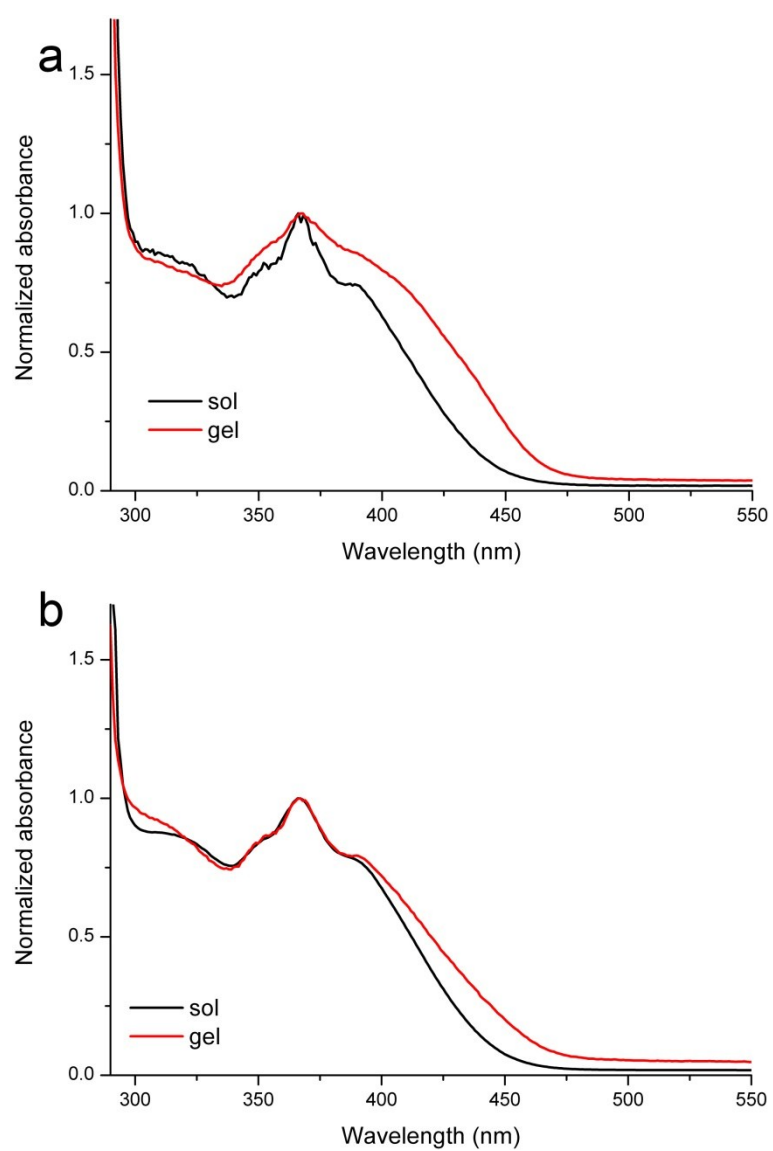


Fig. S3 Normalized UV-vis absorption spectra of PC2VA (a) and PC3VA (a) in sol and gel states.

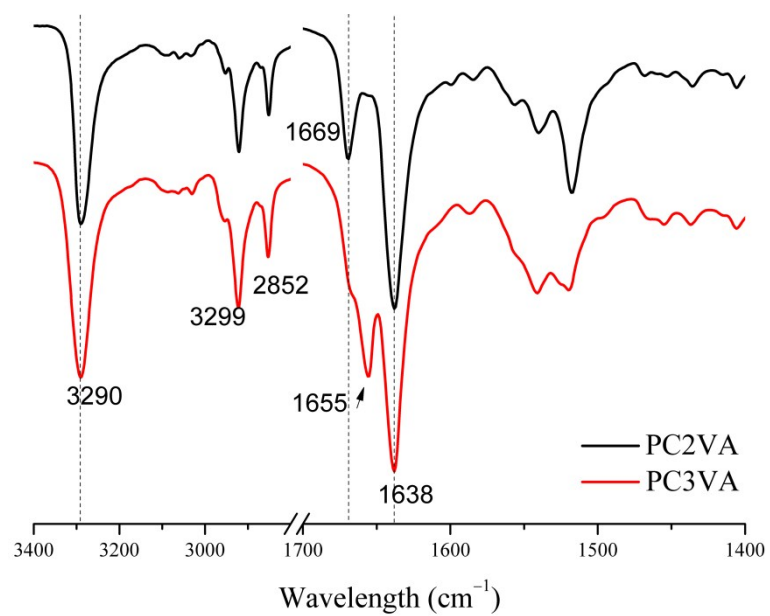


Fig. S4 IR spectra of xerogels of PC2VA and PC3VA ODCB gels.

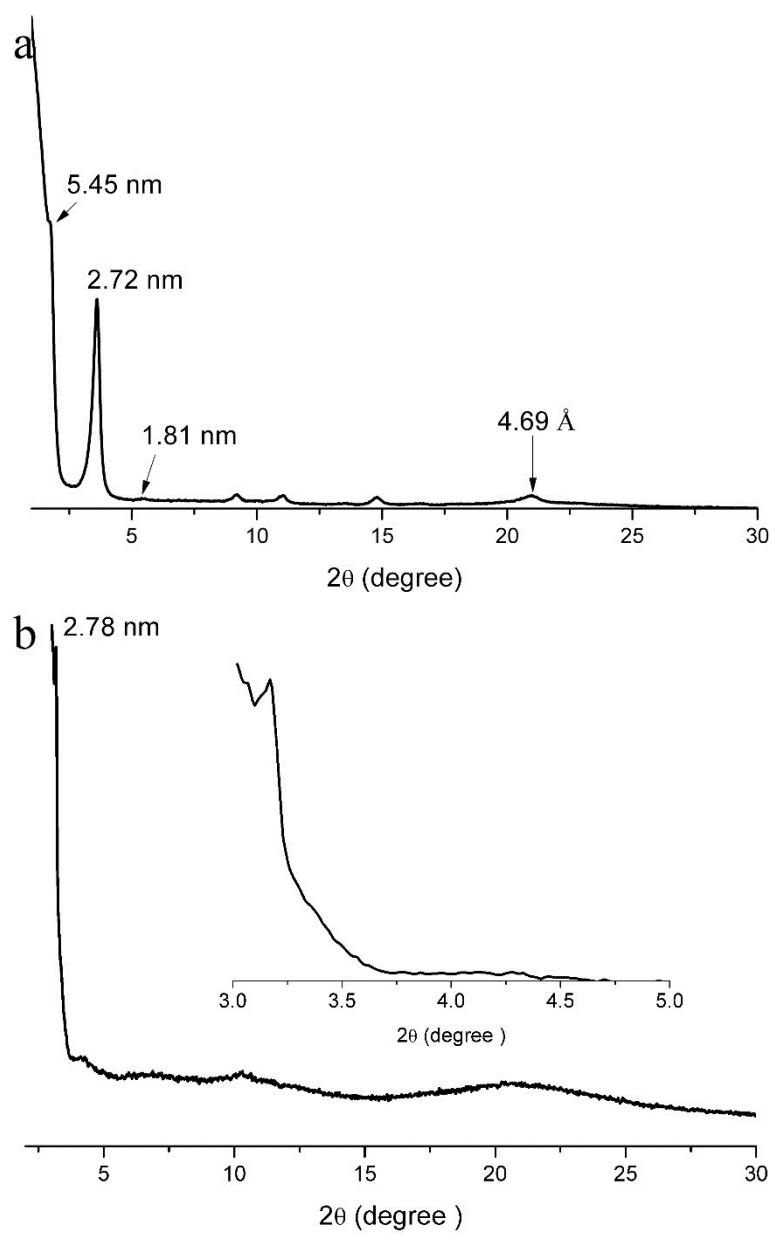


Fig. S5 XRD patterns of PC2VA (a) and PC3VA (b) xerogels.

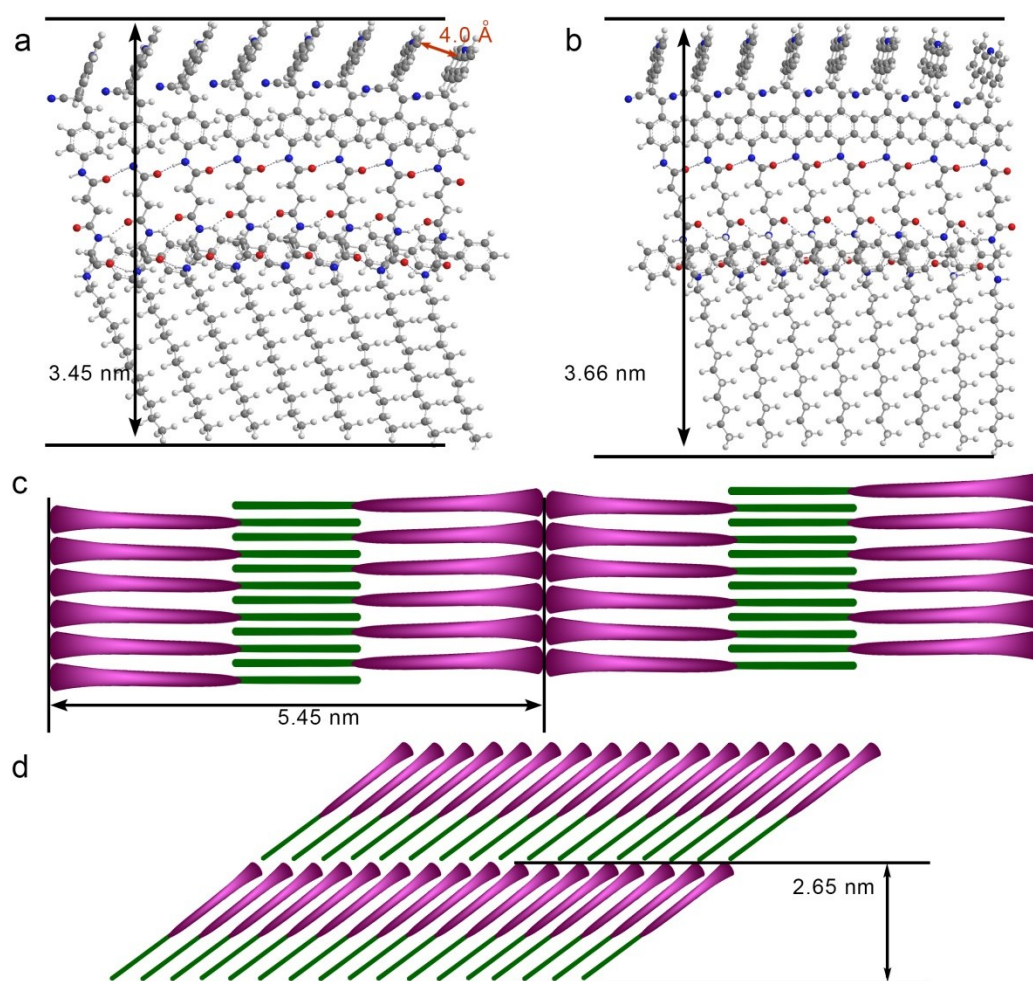


Fig. S6 Molecular packing of PC2VA (a) and PC3VA (b) along with hydrogen bonds obtained by MMFF4 force field minimization. (c) Layer stacking with an interpenetrating bimolecular structure in PC2VA gel, and (d) layer stacking with a tilted arrangement in PC3VA gel.

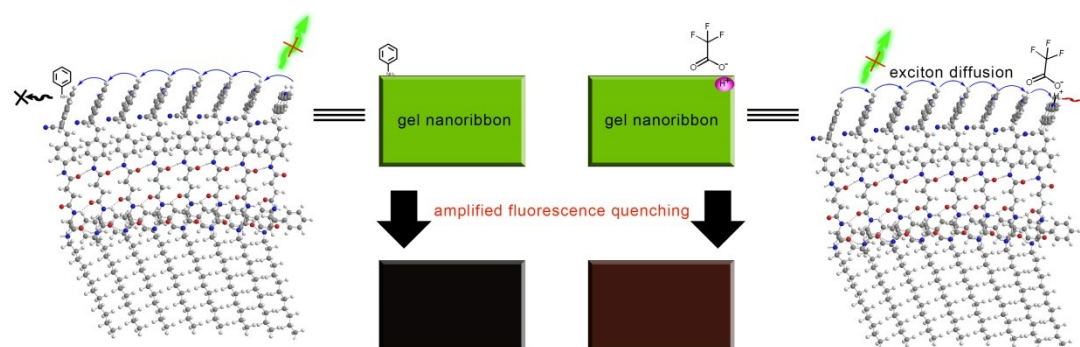


Fig. S7 Response mechanisms of nanoribbons to aniline (left) and TFA (right) in wet gel or gel film.

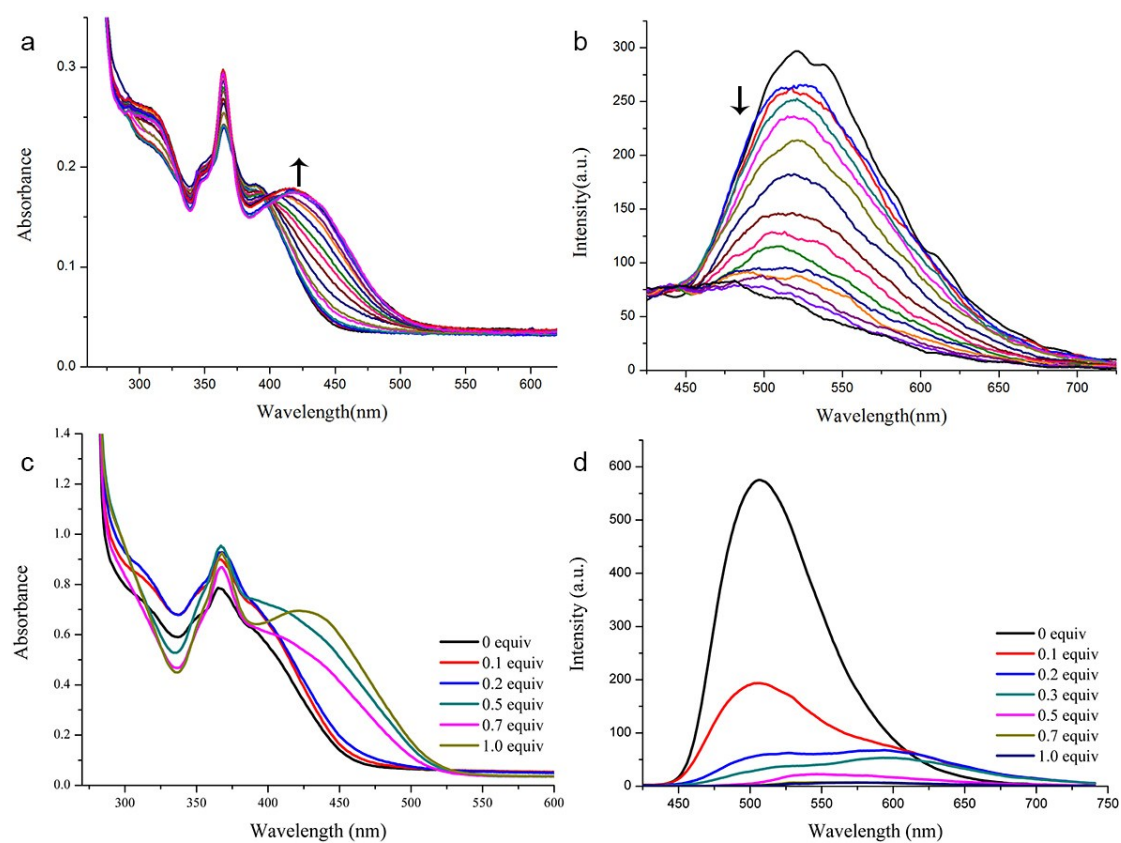


Fig. S8 UV-vis absorption (a and c) and fluorescence (b and d) spectral changes for CHCl_3 solution (a and b, 10^{-5} M) and the CB system (c and d, 1.0 mg/mL) upon addition of TFA. $\lambda_{\text{ex}} = 380$ nm.

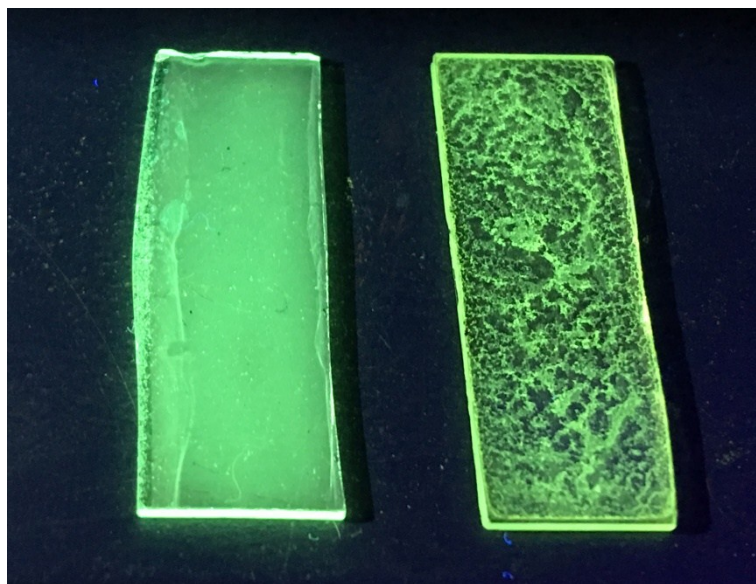


Fig. S9 Photos of PC2VA (left) and PC3VA (right) xerogel films under 365 nm light.

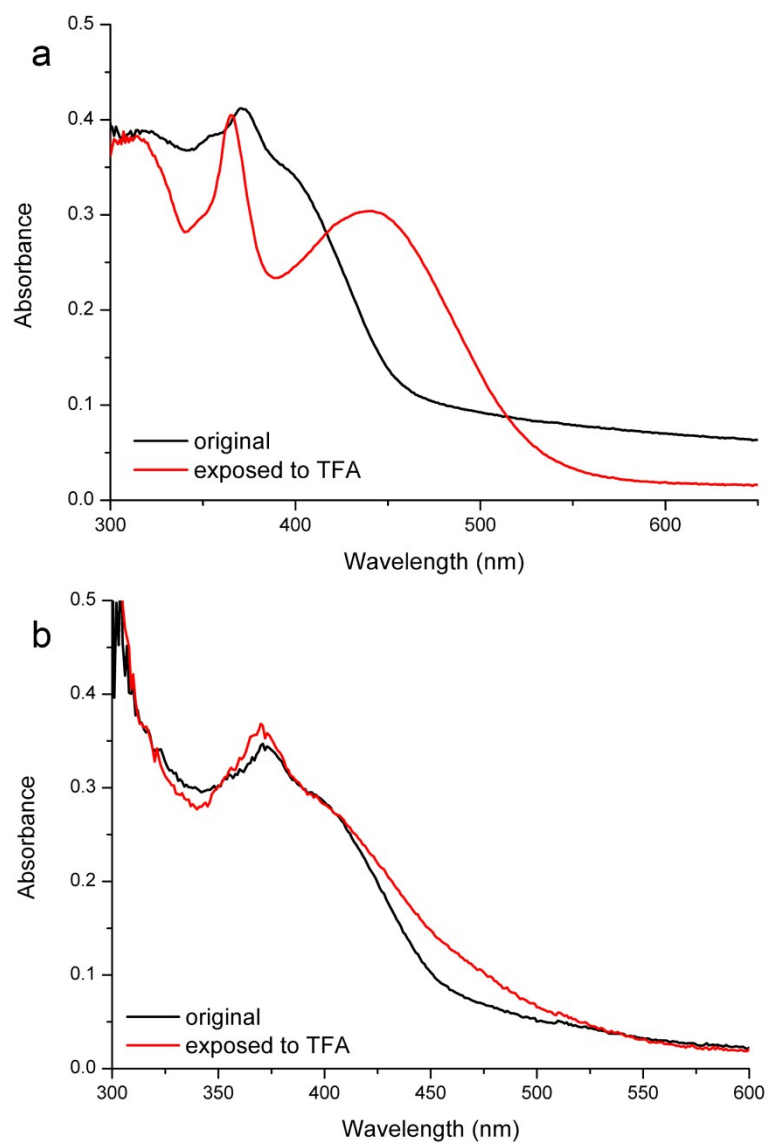


Fig. S10 UV-vis absorption spectra of PC2VA xerogel film after exposing to (a) saturated and (b) 1120 ppm TFA vapor.

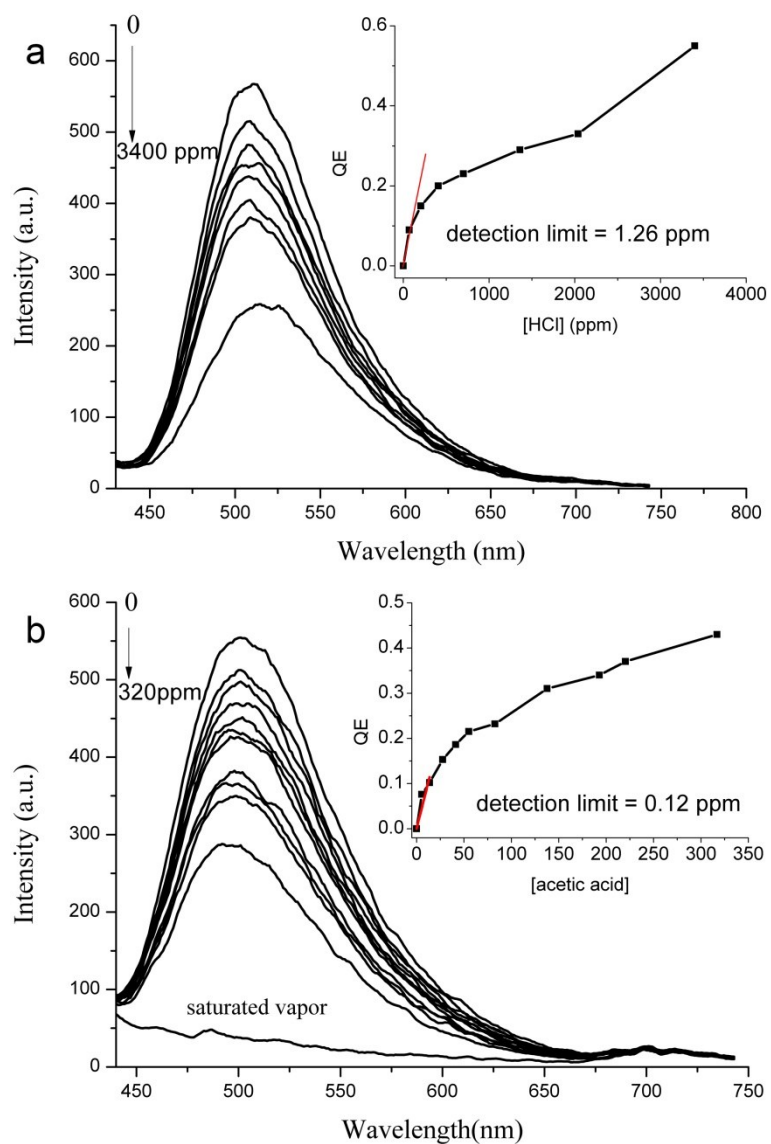


Fig. S11 Fluorescence spectral changes of PC2VA gel films upon exposure to (a) gaseous HCl and (b) acetic acid. Insets: concentration-dependent fluorescence quenching efficiency (QE) of the xerogel film.

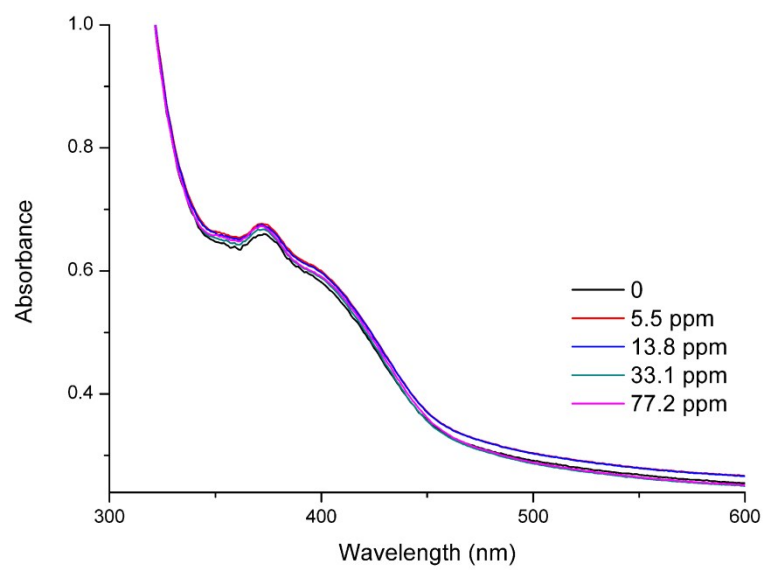


Fig. S12 Absorption spectra of xerogel film exposed to acetic acid vapor.

Table S2. Photophysical data of PC2VA in dry DMF and energy levels obtained by quantum chemical calculation.

| | $\lambda_{\text{abs}}^{\text{a}}$ | $\lambda_{\text{onset}}^{\text{a}}$ | E_{g}^{b} | HOMO ^c | LUMO ^d | HOMO ^e | LUMO ^e |
|-------|-----------------------------------|-------------------------------------|---------------------------|-------------------|-------------------|-------------------|-------------------|
| | (nm) | (nm) | (eV) | (eV) | (eV) | (eV) | (eV) |
| PC2VA | 364, 386 | 441 | 2.81 | -5.73 | -2.92 | -5.68 | -2.45 |

^a Measured in DMF (10^{-5} M); ^b E_{g} was determined from the edge of the absorption spectrum. ^c Obtained by first oxidation peak in DMF with ferrocene/ferrocenium (Fc/Fc^+) as an internal reference. ^d $E_{\text{LUMO}} = E_{\text{HOMO}} + E_{\text{g}}$. ^e DFT calculated at theoretical level of B3LYP/6-31G.

Table S3. The HOMO energy levels of amines.

| Amine | HOMO (eV) | LUMO (eV) | Amine | HOMO (eV) | LUMO (eV) |
|---------------------|--------------|--------------|-----------------|--------------|--------------|
| aniline | -5.63 | -1.56 | cyclohexylamine | -6.46 | -1.31 |
| N-methylaniline | -5.44 | -1.38 | n-butylamine | -6.13 | -0.96 |
| N,N-dimethylaniline | -5.36 | -1.29 | triethylamine | -5.76 | -0.59 |
| phenylhydrazine | -4.36 | -0.36 | PC2VA | -5.73 | -2.92 |

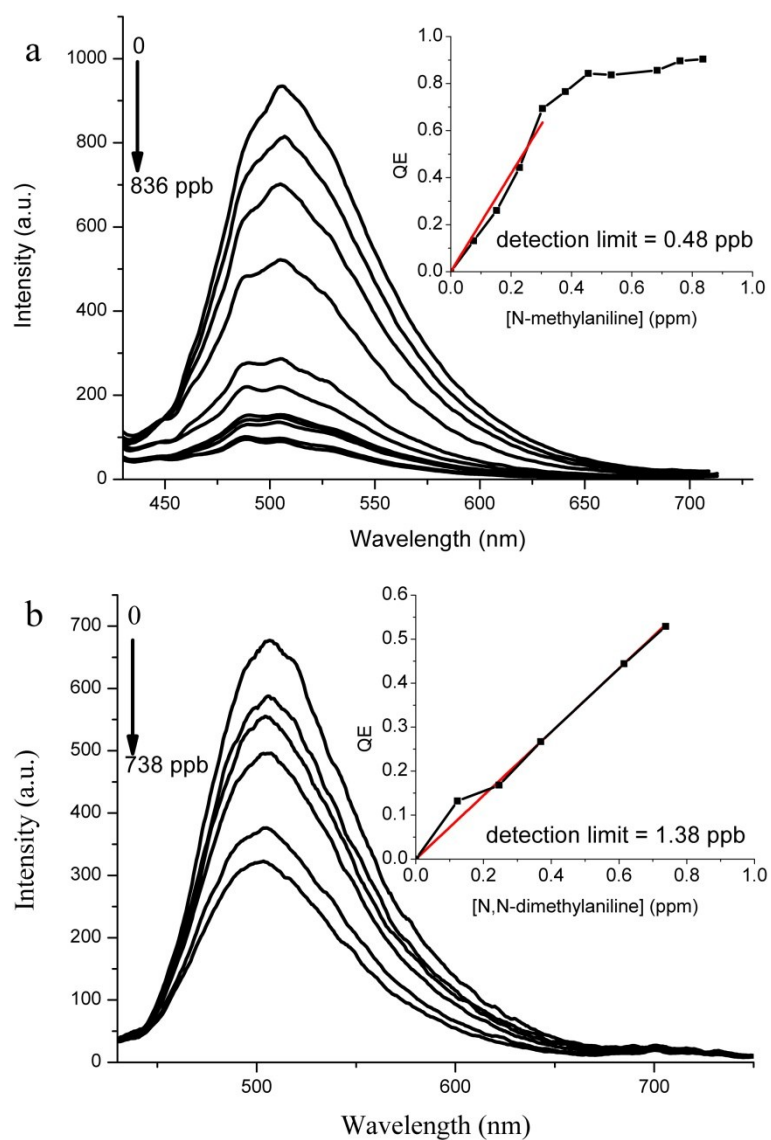


Fig. 13 Fluorescence spectral changes of PC2VA gel films upon exposure to (a) N-methylaniline and (b) N,N-dimethylaniline. Insets: concentration-dependent fluorescence quenching efficiency (QE) of the xerogel film.

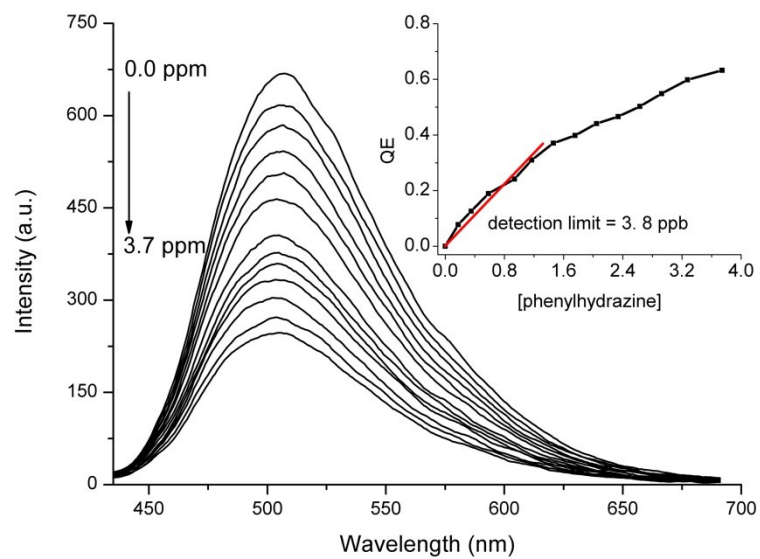


Fig. S14 Fluorescence spectral change of xerogel film exposed to phenylhydrazine vapors. Inset is the plot of QE vs. concentration of phenylhydrazine.

Table S4. Detection limits (DL) and quenching efficiencies (QE) of xerogel film of PC2VA to different vapors.

| | DL | QE (%) ^a | | DL | QE |
|---------------------------------|----------|---------------------|-----------------|----|------|
| aniline | 0.33 ppb | 80 | THF | | 0.01 |
| N-methylaniline | 0.48 ppb | 92 | toluene | - | 0.01 |
| N,N-dimethylaniline | 1.38 ppb | 75 | triethylamine | - | 2.0 |
| phenylhydrazine | 3.8 ppb | 23 | n-butylamine | - | -3.0 |
| acetone | - | 0.16 | cyclohexylamine | - | -11 |
| ethanol | - | -2.3 | NH ₃ | - | 1.0 |
| ethyl acetate | - | 0.1 | tributylamine | - | 4.0 |
| CH ₂ Cl ₂ | - | 1.0 | | | |

^a Concentrations of aniline, N-methylaniline and N,N-dimethylaniline are 1.0 ppm, and those of other analytes are 100 ppm.